Demodulation of Double Differential PSK in Presence of Large Frequency Offset and Wide Filter

Siavash Safapourhajari, André B. J. Kokkeler
University of Twente, Netherlands
Email: s.safapourhajari@utwente.nl, a.b.j.kokkeler@utwente.nl

***Abstract*—The autocorrelation demodulator (ACD) for DDPSK is an offset tolerant demodulator which has been introduced for applications where the signal experiences large Doppler shift. Moreover, emerging ultra-narrowband solutions for Internet of Things and Wireless Sensor Networks can exploit DDPSK to avoid the use of costly crystal or power hungry thermal compensators. However, to tolerate frequency offset the bandwidth of the lowpass or bandpass filter before the demodulator must increase which leads to a larger noise bandwidth and degrades BER performance. This work proposes a new method to overcome this problem. Instead of one path of ACD, samples at the output of the filter go through multiple paths with adjusted delay and interval for correlation in the ACD. The sum of the outputs of these paths provide the input to the detector with an increased SNR compared to conventional structure. Using the proposed method, the SNR per bit required for a certain BER remains independent of filter bandwidth if the target BER is less than 0.01.**

I. Introduction

Autocorrelation demodulation (ACD) of second-order differential PSK also known as Double Differential PSK (DDPSK) is a demodulation method independent of frequency offset [1]. In low data rate applications, where Doppler shift reaches up to multiple times the data rate, offset tolerant demodulation has been utilized as an interesting solution. It removes carrier recovery which takes long time and consumes considerable power in these scenarios [2], [3]. Moreover, it can be applied in ultra-narrowband (UNB) schemes for Internet of Things (IoT) and Wireless Sensor Network (WSN) applications where the frequency offset challenge becomes crucial. In these systems a frequency offset equal to a fraction of the data rate (which then can be estimated and compensated in the digital domain) necessitates a costly crystal with thermal compensation [4]. A frequency offset tolerant demodulator can be a solution in order to avoid extra cost and power consumption.

Simplified carrier recovery for DDPSK receiver comes at the cost of loss in BER performance. Various methods have been proposed to improve BER performance of DDPSK. In [5], a multiple symbol detection (MSD) scheme for DPSK [6] is utilized to improve BER performance. Deriving a MAP detector metric, a decision feedback based multiple symbol detection is introduced in [7]. In [8] and [9] three methods for MSD in DDPSK are compared and it is concluded that the simple method suggested in [5] is the best as the huge complexity added by other methods overweighs their BER performance gain which is less than 0.5 dB.

In addition to offset tolerant demodulation in the receiver, the bandwidth of the filter before the demodulator should increase in accordance with expected frequency offset. Otherwise, the frequency offset pushes the signal out of the filter. On the other hand, as the noise bandwidth is proportional to the filter bandwidth, BER performance deteriorates in presence of a wide filter [5]. In low data rate applications where Doppler shift exists the frequency offset may range from 10 to 100 times the data rate [3]. Despite efforts to improve the BER performance of DDPSK, the mentioned techniques suffer from performance degradation in presence of a wide filter and their BER performance is dependent on filter bandwidth.

In this paper a novel method is proposed to overcome the effect of a wide filter in DDPSK. The only requirement is that the sample rate after the filter must be the same as the filter bandwidth so that the noise samples are uncorrelated. The proposed method can effectively reduce the effect of noise included by the wide filter at the cost of additional digital complexity. As a result, the BER performance of the proposed demodulator is independent of the filter bandwidth. In addition to simulations, a mathematical approach is followed to analyze noise components and prove effectiveness of the proposed method. Before explicating the proposed method, a conventional ACD for DDPSK is briefly explained in the next section and the problem is defined. Section III elaborates on the proposed method and its BER performance. Simulation results are presented in section IV while conclusions are drawn in section V.

II. Conventional ACD and problem statement

The block diagram of a double differential encoder together with conventional autocorrelation demodulator (ACD) for double differential PSK are shown in Fig.1. The double differential encoder is composed of two differential encoders in series. In the receiver, the samples of the double differentially encoded signal are filtered and pass through two consecutive differential decoders. The first stage of the ACD converts the frequency offset to a constant phase offset by correlating each symbol with the previous symbol. Subsequently, the second stage removes the remaining phase offset [1]. Thus, the output d_n of the demodulator is independent of frequency offset.

A simple modification to DDPSK achieved without additional complexity was introduced in [5]. It is obtained by increasing the delay of the second stage of the encoder and the first stage of the demodulator in Fig. 1 by one symbol period

978-1-5386-6355-4/18/$31.00

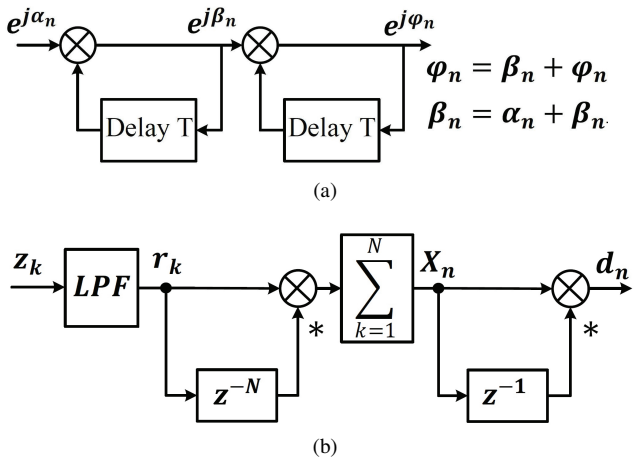

Fig. 1. (a) Block diagram of double differential encoder with phase relations and (b) ACD for DDPSK, T is symbol period and N is the number of samples per symbol and $(*)$ denotes complex conjugate

(changing them to $2T$ and $2N$, respectively). This method, denoted by 2T-DDPSK improves the BER performance as it decreases correlation between noise samples in the two stages [5].

Considering an approach similar to [5], it is assumed that the signal passes through a low pass filter with single side bandwidth F before the demodulator. In case of an ideal filter and neglecting ISI for a signal with zero frequency offset, the filter bandwidth can be $F = 1/T$ where T is symbol period [5]. In presence of frequency offset a wider filter ($F > 1/T$) is required and the BER performance declines. The proposed method aims at overcoming the impact of a wider filter on DDPSK via modifying the autocorrelation stage. The proposed method is explained for DDPSK but it can be directly used in case of 2T-DDPSK. In the next section, first, improvement of a single-stage autocorrelation demodulator is explicated. Thereafter, the same idea is exploited to design a demodulator for double differential detection.

III. The Proposed Demodulator

A. Single-Stage ACD

The proposed demodulator is designed for DDPSK since the issue of a large filter will be a concern only when the demodulator is supposed to afford large frequency offset. A single-stage ACD is, in fact, a DPSK demodulator (and not a DDPSK demodulator) which just eliminates phase offset. Nevertheless, it is elaborated here to clarify the proposed idea. In the following, it is assumed that the single side bandwidth of the filter (F) is a multiple of the data rate, similar to [5]. The minimum sampling rate after the filter must be F (according to the Nyquist theorem) for complex samples. Thus, there are $N = FT$ complex samples per symbol after filter and at the input of ACD. Considering an AWGN channel, such a sampling frequency ensures that noise samples are white circularly symmetric Gaussian random variables. The baseband equivalent of samples for a DPSK signal during the n^{th} symbol is:

$$r_{k,n} = s_{k,n}e^{j\theta} + \eta_{k,n} \tag{1}$$

Where $r_{k,n}$ is the k^{th} sample from the n^{th} symbol ($k = 1, ..., N$); considering rectangular pulse shaping and neglecting ISI (which is reasonable for large F) $s_{k,n} = s_n = e^{j2\pi i/M}$, $i = 1, 2, , M-1$ for MPSK; θ is phase offset and $\eta_{k,n}$ for all k are independent circularly symmetric Gaussian random variables. Here, just the phase offset is included in the model and frequency offset is assumed to be zero. In a conventional demodulator the received samples of consecutive symbols are correlated over a symbol period. This provides the output of the ACD as follows.

$$X_n = \sum_{k=1}^{N} r_{k,n} r^*_{k,n-1} \tag{2}$$

Now, let us define $X^R_{n,p}$ and $X^L_{n,p}$ as:

$$X^R_{n,p} = \sum_{k=p+1}^{N} r_{k,n} r^*_{k-p,n-1} \tag{3}$$

$$X^L_{n,p} = \sum_{k=1}^{N-p} r_{k,n} r^*_{k+p,n-1} \tag{4}$$

This can be interpreted as increasing and decreasing (respectively for $X^R_{n,p}$ and $X^L_{n,p}$) the delay of N samples in Fig. 1 while adjusting the limits of summation to make sure that each term in the summation corresponds to the same pair of symbols. It is, indeed, adding duplicate paths of correlation between signal and its delayed version with adjusted delay and summation blocks. In the proposed method for single-stage ACD, the decision is made based on the sum of all $X^{R(L)}_{n,p}$ ($X^R_{n,p}$ or $X^L_{n,p}$) values and X_n denoted by $X_{n,Tot}$.

$$X_{n,Tot} = X_n + \sum_{p=1}^{N-1} (X^R_{n,p} + X^L_{n,p}) \tag{5}$$

According to (1) since $s_{k,n}$ is equal for all k in a symbol, the individual signal components in X_n and all $X^{R(L)}_{n,p}$ are the same and just dependent on the phase difference between two consecutive symbols. In $X_{n,Tot}$, signal components are added coherently while noise components are added incoherently. Therefore, the effective SNR increases leading to better BER performance. If $X^{R(L)}_{n,p}$ values are calculated and added together for all $p = 1, 2, ..., N-1$, the BER performance will be exactly the same as in the $FT = 1$ case for arbitrarily large N. This is shown in the next subsection.

B. Error Probability

It is difficult (if not impossible) to derive a closed form expression for the error probability of the proposed method. Therefore, to prove the effectiveness of the above method, an alternative approach is adopted. The signal and noise components of $X_{n,Tot}$ are modeled. Then, the ratio of the signal power to the power of each noise component is calculated for $FT = 1$ and $FT = N$. As the distributions of noise components are the same in both cases (it is shown in the sequel), equal signal to noise ratio is equivalent to similar error probability. First, the two basic assumptions are repeated:

(I). The sampling frequency equals F for each real and imaginary part ($FT = N$ complex samples per symbol). This means that all noise samples ($\eta_{k,n}$) are independent circularly symmetric Gaussian noise $\mathcal{CN}(0, \sigma^2)$ i.e. $Re\{\eta_{k,n}\}$ and $Im\{\eta_{k,n}\}$ are independent Gaussian random variables $N(0, \sigma^2/2)$.

(II). Rectangular pulse shaping is assumed and ISI is ignored which is reasonable when FT is large. So the signal component of all samples in a symbol are the same.

Using the signal model (1) and replacing terms within (5) with their expansions, after simple manipulations we have:

$$X_{n,Tot} = S_{Tot} + (H_s)_{Tot} + (H_\eta)_{Tot} \tag{6}$$

Where S_{Tot} is signal component while $(H_s)_{Tot}$ and $(H_\eta)_{Tot}$ are two noise components resulting from signal-by-noise and noise-by-noise multiplication, respectively. These three components in (6) are as follows:

$$\begin{aligned} S_{Tot} &= \sum_{k=1}^{N} s_{k,n} s^*_{k,n-1} \\ &\quad + \sum_{p=1}^{N-1} \Big(\sum_{k=p+1}^{N} s_{k,n} s^*_{k-p,n-1} + \sum_{k=1}^{N-p} s_{k,n} s^*_{k+p,n-1} \Big) \\ &= N^2 s_n s^*_{n-1} \end{aligned} \tag{7}$$

$$\begin{aligned} (H_s)_{Tot} &= \sum_{k=1}^{N} (s_{k,n}\eta^*_{k,n-1} + s^*_{k,n-1}\eta_{k,n}) \\ &\quad + \sum_{p=1}^{N-1} \sum_{k=p+1}^{N} (s_{k,n}\eta^*_{k-p,n-1} + s^*_{k-p,n-1}\eta_{k,n}) \\ &\quad + \sum_{p=1}^{N-1} \sum_{k=1}^{N-p} (s_{k,n}\eta^*_{k+p,n-1} + s^*_{k+p,n-1}\eta_{k,n}) \\ &= \sum_{k=1}^{N} N s^*_{n-1}\eta_{k,n} + \sum_{k=1}^{N} N s_n \eta^*_{k,n-1} \end{aligned} \tag{8}$$

$$\begin{aligned} (H_\eta)_{Tot} &= \sum_{k=1}^{N} \eta_{k,n}\eta^*_{k,n-1} + \sum_{p=1}^{N-1} \sum_{k=p+1}^{N} \eta_{k,n}\eta^*_{k-p,n-1} \\ &\quad + \sum_{p=1}^{N-1} \sum_{k=1}^{N-p} \eta_{k,n}\eta^*_{k+p,n-1} \\ &= \sum_{k=1}^{N} \sum_{i=1}^{N} \eta_{i,n}\eta^*_{k,n-1} \end{aligned} \tag{9}$$

As a result of assumption (I) all individual terms within (8), namely, $N s^*_{n-1}\eta_{k,n}$ and $N s_n \eta^*_{k,n-1}$ are independent circularly symmetric Gaussian random variables $\mathcal{CN}(0, N^2\sigma^2)$; thus, $(H_s)_{Tot}$ is $\mathcal{CN}(0, 2N^3\sigma^2)$. In $(H_\eta)_{Tot}$, all terms $(\eta_{i,n}\eta^*_{k,n-1})$ are also independent complex random variables where the real and imaginary parts have the same distribution. In $Re\{(H_\eta)_{Tot}\}$ each component can be written as follows:

$$Re\{\eta_{i,n}\eta^*_{k,n-1}\} = \eta^{Re}_{i,n}\eta^{Re}_{k,n-1} + \eta^{Im}_{i,n}\eta^{Im}_{k,n-1} \tag{10}$$

Where the superscripts Re and Im denote real part and imaginary part, respectively. $\eta^{Re}_{i,n}$, $\eta^{Re}_{k,n-1}$, $\eta^{Im}_{i,n}$ and $\eta^{Im}_{k,n-1}$ are independent Gaussian random variables ($N(0, \sigma^2/2)$) according to assumption (I). To obtain the distribution of the product of two independent Gaussian random variables x and y with zero mean and similar variance (σ^2_x), xy can be written as $xy = (x+y)^2/4 - (x-y)^2/4$ where $x+y$ and $x-y$ are independent Gaussian variables with zero mean and $2\sigma^2_x$ variance. The square of such a Gaussian random variable has a Gamma distribution with shape and rate parameters equal to $1/2$ and $1/\sigma^2_x$, respectively ($\Gamma(1/2, 1/\sigma^2_x)$) [10]. Thus, the two terms of xy are independent Gamma distributed random variables $\Gamma(1/2, 4/\sigma^2_x)$. Moreover, the sum of two Gamma random variables, $\Gamma(\alpha_1, \beta)$ and $\Gamma(\alpha_2, \beta)$, is a Gamma random variable with shape parameter $\alpha 1 + \alpha 2$ and rate parameter β, ($\Gamma(\alpha 1 + \alpha 2, \beta)$) [10]. Considering the distribution of the components in (10) (which is $N(0, \sigma^2/2)$) and the above calculations, $Re\{\eta_{i,n}\eta^*_{k,n-1}\}$ is the difference of two independent random variables with a $\Gamma(1, 8/\sigma^2)$ distribution. Hence, $Re\{(H_\eta)_{Tot}\}$ is obtained as:

$$Re\{(H_\eta)_{Tot}\} = \sum_{i=1}^{N^2} R_i - \sum_{i=1}^{N^2} Q_i \tag{11}$$

where R_i and Q_i are independent random variables with Gamma distribution ($R_i, Q_i \sim \Gamma(1, 8/\sigma^2)$). Consequently, the distribution of $Re\{(H_\eta)_{Tot}\}$ will be equal to difference of two independent random variables with $\Gamma(N^2, 8/\sigma^2)$ distribution. The difference between two independent Gamma random variables $\Gamma(1/\lambda, 1/\sqrt{\lambda\theta})$ is a random variable with Double Gamma Difference ($DGD(\lambda, \theta)$) distribution with a variance of 2θ [11]. So, the overall distribution of $Re\{(H_\eta)_{Tot}\}$ is a Double Gamma Difference distribution, $DGD(1/N^2, N^2\sigma^4/64)$. The variance (power) of the noise component with such a distribution is $N^2\sigma^4/32$. Doing similar calculations, $Im\{(H_\eta)_{Tot}\}$ also has a $DGD(1/N^2, N^2\sigma^4/64)$ distribution. Since the real and the imaginary parts are independent, the total power of $(H_\eta)_{Tot}$ is $N^2\sigma^4/16$. Following the same procedure, the power of the noise components for $FT = 1$ are $2\sigma^2_1$ and $\sigma^4_1/16$ for $(H_s)_{Tot}$ and $(H_\eta)_{Tot}$, respectively, where σ^2_1 is the noise power (at the input of ACD) when the filter bandwidth is $1/T$ ($FT = 1$).

According to (7), the Power of the signal component in $X_{n,Tot}$ when $FT = N$ is N^4 times its value in the $FT = 1$ case. Besides, it is clear that $\sigma^2 = N\sigma^2_1$ (for $FT = N$, the noise spectral density is the same while its bandwidth is multiplied by N). Taking all aforementioned into account, we have the following equations for the SNR corresponding to different noise components in the proposed decision variable when $FT = N$:

$$SNR_{H_s} = \frac{N^4 P_{s,1}}{2N^3(N\sigma^2_1)} = \frac{P_{s,1}}{2\sigma^2_1} \tag{12}$$

$$SNR_{H_\eta} = \frac{N^4 P_{s,1}}{N^2\sigma^4/16} = \frac{P_{s,1}}{\sigma^4_1/16} \tag{13}$$

Where $P_{s,1}$ is the power of the signal component in $X_{n,Tot}$ when $FT = 1$. As can be seen, the SNR corresponding to both noise components ($(H_s)_{Tot}$ and $(H_\eta)_{Tot}$) in the proposed

method when $FT = N$ are the same as SNR values in case of $FT = 1$. It means that the BER performance for the proposed method is equal for both $FT = 1$ and $FT = N$. To clarify the difference between the proposed method and the conventional method, the SNR values corresponding to both noise components in the output of a conventional single-stage ACD with $FT = N$ are calculated. In this case $p = 0$ and there is only one path so the output is simply equal to X_n .

$$SNR_{H_s} = \frac{N^2 P_{s,1}}{2N(N\sigma_1^2)} = \frac{P_{s,1}}{2\sigma_1^2} \tag{14}$$

$$SNR_{H_\eta} = \frac{N^2 P_{s,1}}{N\sigma^4/16} = \frac{P_{s,1}}{N\sigma_1^4/16} \tag{15}$$

As shown by (15), the ratio of signal power to the power of $(H_\eta)_{Tot}$ for the proposed method (see (13)) is N times of that for conventional single-stage ACD. However, as clarified by (12) and (14) this ratio for $(H_s)_{Tot}$ is the same for the proposed method as for the conventional method. In fact, in the proposed method the individual H_s components that are summed are completely correlated while the H_η components are uncorrelated. As can be seen in (14), even for conventional ACD, SNR_{H_s} is equal for both $FT = 1$ and $FT = N$. In other words, H_η (and not H_s) is responsible for the difference in BER performance for various FT values and the proposed method removes the effect of this component.

C. The Proposed ACD for DDPSK

The block diagram of the proposed demodulator for DDPSK is depicted in Fig. 2. Although in single-stage ACD, all $X_{n,p}^R$ and $X_{n,p}^L$ values are added together to form the ultimate output of the demodulator, these values for DDPSK cannot be simply added and fed to the next stage of differential demodulation (second stage of ACD). The reason is the different phase offset in the signal component for each path resulting from frequency offset. To solve this problem, it is necessary to first apply the second differential decoder to each $X_{n,p}^{R(L)}$ (to each path in Fig. 2) so that the additional phase offset is removed. Then, the results can be simply added together to form the final output of the demodulator, which is $d_{n,Tot}$. Considering (1) and an expansion similar to (6) for each $X_{n,p}^{R(L)}$, the output of each path ($d_{n,p}^{R(L)}$) has nine components. For large SNR, the terms including multiplication of noise components resulting from first stage ($H_s H_\eta$ and $H_\eta H_\eta$) are negligible (as the power of noise sample in them is more than two); thus, $d_{n,p}^R$ and $d_{n,p}^L$ can be approximated as follows:

$$\begin{aligned} d_{n,p}^{R(L)} \approx\ & S_{n,p}^{R(L)} S_{n-1,p}^{R(L)} \\ & + S_{n,p}^{R(L)} ((H_s)_{n-1,p}^{R(L)})^* + (S_{n-1,p}^{R(L)})^* (H_s)_{n,p}^{R(L)} \\ & + S_{n,p}^{R(L)} ((H_\eta)_{n-1,p}^{R(L)})^* + (S_{n-1,p}^{R(L)})^* (H_\eta)_{n,p}^{R(L)} \end{aligned} \tag{16}$$

Where $S_{n,p}^{R(L)}$, $(H_s)_{n,p}^{R(L)}$ and $(H_\eta)_{n,p}^{R(L)}$ are signal, signal-by-noise and nois-by-noise components of $X_{n,p}^{R(L)}$, respectively. As shown before, the proposed method does not affect SNR_{H_s}, so only the effect of noise components with H_η is analyzed here. The rest of the mathematical calculations focus

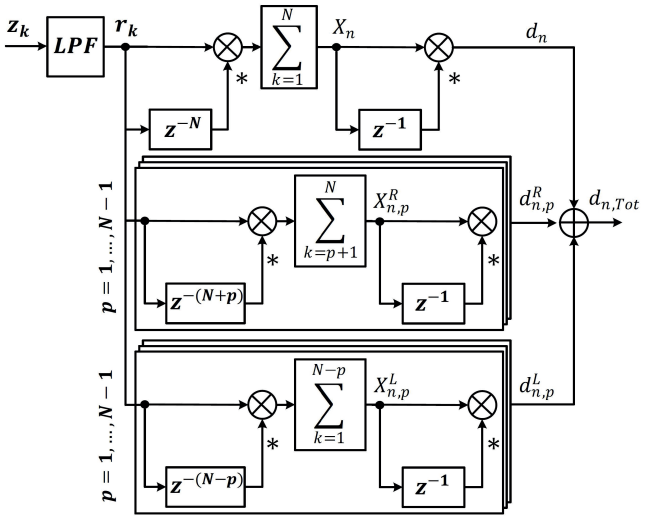

Fig. 2. Block diagram of the proposed demodulator for DDPSK

on the sum of $S_{n,p}^{R(L)}((H_\eta)_{n-1,p}^{R(L)})^*$ components (denoted by $S \times H_\eta^*$) and the same can be derived for $(S_{n-1,p}^{R(L)})^*(H_\eta)_{n,p}^{R(L)}$. Since $S_{n,p}^{R(L)} = (N-p)s_n s_{n-1}^* \triangleq (N-p)z_n$, the corresponding noise component in the demodulator output is:

$$\begin{aligned} S \times H_\eta^* = N z_n (H_\eta)_n + \sum_{p=1}^{N-1} z_n (N-p)((H_\eta)_{n,p}^R)^* \\ + \sum_{p=1}^{N-1} z_n (N-p)((H_\eta)_{n,p}^L)^* \end{aligned} \tag{17}$$

As explained before, all $\eta_{k,n}\eta_{i,n-1}^*$ are independent random variables so $((H_\eta)_{n,p}^{R(L)})^*$ for each p are complex random variables (DGD distirbution for real and imaginary parts) with a variance of $(N-p)\sigma^4/16$. As the signal component, $z_n(N-p)$, is a constant complex number, where $z_n z_n^* = 1(1)$, the variance of each term inside the sum over p would be $(N-p)^3\sigma^4/16$. All terms in the right hand side of (17) are independent, so the total power is:

$$P_{(S\times H_\eta^*)} = \frac{N^2(N^2+1)}{2}\frac{\sigma^4}{16} \tag{18}$$

The signal component in $d_{n,Tot}$ which is the final output of demodulator (sum of all paths) equals to:

$$S_{(d_{n,Tot}),FT=N} = z_n z_{n-1}^* (N^2 + 2\sum_{p=1}^{N-1}(N-p)^2) \tag{19}$$

With a simple calculation it can be seen that the signal power in the output of the proposed demodulator is $N^2(2N^2+1)^2/9$ times of the signal power for $FT = 1$. As a result, the ratio of the SNR corresponding to the $S\times H_\eta^*$ component for $FT = N$ and $FT = 1$ can be calculated as:

$$\frac{SNR_{S\times H_\eta^*, FT=N}}{SNR_{S\times H_\eta^*, FT=1}} = \frac{8N^4+8N^2+2}{9N^4+9N^2} \tag{20}$$

The limit of the above ratio when N approaches to infinity is 0.89 while for $N = 2$ this ratio is 0.9. Using only X_n

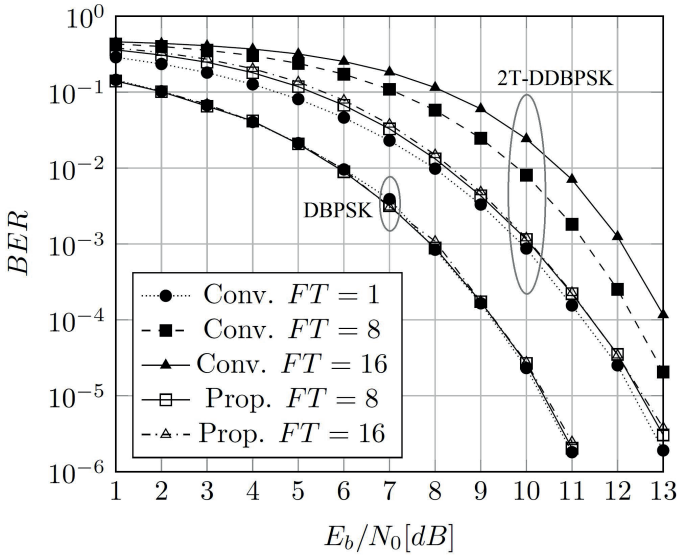

Fig. 3. BER performance of the proposed method for DBPSK and 2T-DDBPSK

as the output and similar to (15) the same ratio (as in (20)) for conventional DDPSK will be equal to $1/N$. Although $SNR_{S\times H_\eta^*,FT=N}$ for the proposed method is not completely matched to the case of $FT = 1$, it is much higher than its value for the conventional method. This higher SNR leads to improved BER performance of the proposed method. Besides, the minimum SNR, related to the discussed noise components for the proposed demodulator equals 0.89 of its value for $FT = 1$ even in case of arbitrarily large N.

IV. Simulation Results

Similar to [5], BER curves are presented for different values of FT which is the filter bandwidth normalized to symbol rate. Fig. 3 depicts BER curves for binary DPSK (DBPSK) and binary DDPSK (DDBPSK) using the proposed method for $FT = 1, 8, 16$. In case of DBPSK, the BER curves for all FT values exactly match the BER curve for $FT = 1$ which is equal for both the conventional and the proposed demodulators. For binary DDPSK, the proposed method is applied to 2T-DDBPSK and the results are shown for $FT = 1, 8, 16$. To demonstrate the improvement achieved by the proposed method in case of DDBPSK, BER curves of a conventional demodulator for $FT = 8, 16$ are illustrated. It can be seen that for $FT = 16$ and $BER = 10^{-3}$ more than $2dB$ improvement is obtained. The slight difference in BER performance for various FT values in the very low SNR region is caused by the terms generated by higher powers of noise. These are the same noise components neglected in our calculations in previous section. For higher SNR, the effect of these values decreases such that the BER curves get closer to that of $FT = 1$. The small deviation from $FT = 1$ which remains even for large SNR is due to the 11% decrease in the $SNR_{S\times H_\eta^*,FT=N}$ (compared to $FT = 1$ case) which was shown in previous section. The loss for all FT values is less than 0.3 dB when a BER less than 10^{-2} is the target.

V. Conclusion

The BER performance of the autocorrelation demodulator (ACD) for DDPSK in presence of large frequency offset was considered. The bandwidth of the filter before the demodulator should be selected according to the target range for frequency offset tolerance. Although DDPSK is able to tolerate frequency offset, the wide filter required in presence of large frequency offset includes more noise which leads to BER performance degradation. The proposed demodulator adds additional paths to the conventional DDPSK demodulator and the sum of demodulated signals in these paths is sent to the detector. As shown, the proposed method increases SNR at the input of the detector and compensates for SNR loss resulting from the wider filter. Therefore, the BER performance remains unchanged for all values of the filter bandwidth. The simulation results revealed that the proposed method leads to more than 2dB improvement in E_b in case the single side bandwidth of the filter is 16 times the data rate. For wider filters i.e. wider range of frequency offset tolerance, this gain is increasing. In the proposed method, improvement is achieved at the cost of higher digital complexity. However, it reduces the transmit power which is a considerable power saving in a wireless communication link. Moreover, it eliminates the requirement for a thermal compensated and costly crystal, making it possible to have a low power and cheap receiver for WSN applications.

References

[1] M. Simon, S. Hinedi, and W. Lindsey, *Digital Communication Techniques: Signal Design and Detection*. PTR Prentice Hall, 1995.

[2] A. Kajiwara, "Mobile satellite CDMA system robust to Doppler shift," *IEEE Transactions on Vehicular Technology*, vol. 44, no. 3, pp. 480–486, Aug 1995.

[3] M. R. Yuce and W. Liu, "A low-power multirate differential PSK receiver for space applications," *IEEE Transactions on Vehicular Technology*, vol. 54, no. 6, pp. 2074–2084, Nov 2005.

[4] D. Lachartre, F. Dehmas, C. Bernier, C. Fourtet, L. Ouvry, F. Lepin, E. Mercier, S. Hamard, L. Zirphile, S. Thuries, and F. Chaix, "A TCXO-less 100hz-minimum-bandwidth transceiver for ultra-narrow-band sub-GHz IoT cellular networks," in *2017 IEEE International Solid-State Circuits Conference (ISSCC)*, Feb 2017, pp. 134–135.

[5] M. K. Simon and D. Divsalar, "On the implementation and performance of single and double differential detection schemes," *IEEE Transactions on Communications*, vol. 40, no. 2, pp. 278–291, Feb 1992.

[6] D. Divsalar and M. K. Simon, "Multiple-symbol differential detection of MPSK," *IEEE Transactions on Communications*, vol. 38, no. 3, pp. 300–308, Mar 1990.

[7] D. W. Jang and T. H. Choi, "Decision feedback-based demodulation of doubly differential PSK signals," *IEEE Transactions on Communications*, vol. 48, no. 8, pp. 1253–1256, Aug 2000.

[8] P. Stoica, J. Liu, J. Li, and M. A. Prasad, "The heuristic, GLRT, and MAP detectors for double differential modulation are identical," *IEEE Transactions on Information Theory*, vol. 51, no. 5, pp. 1860–1865, May 2005.

[9] M. Simon, J. Liu, P. Stoica, and J. Li, "Multiple-symbol double-differential detection based on least-squares and generalized-likelihood ratio criteria," *IEEE Transactions on Communications*, vol. 52, no. 1, pp. 46–49, Jan 2004.

[10] K. Krishnamoorthy, *Handbook of statistical distributions with applications*. CRC Press, 2016.

[11] M. Augustyniak and L. G. Doray, "Inference for a leptokurtic symmetric family of distributions represented by the difference of two gamma variates," *Journal of Statistical Computation and Simulation*, vol. 82, no. 11, pp. 1621–1634, 2012.